

Peroxymonosulfate Activation by Photoelectroactive Nanohybrid Filter towards Effective Micropollutant Decontamination

Wenchang Zhao ¹, Yuling Dai ², Wentian Zheng ² and Yanbiao Liu ^{2,*}

¹ Fujian Provincial Key Laboratory of Featured Materials in Biochemical Industry, College of Chemistry and Materials, Ningde Normal University, Ningde 352100, China; wenchangzhao@foxmail.com

² Textile Pollution Controlling Engineering Center of Ministry of Environmental Protection, College of Environmental Science and Engineering, Donghua University, Shanghai 201620, China; 2202084@mail.dhu.edu.cn (Y.D.); 2191678@mail.dhu.edu.cn (W.Z.)

* Correspondence: yanbiaoliu@dhu.edu.cn; Tel.: +86 21 67798752

Citation: Zhao, W.; Dai, Y.; Zheng, W.; Liu, Y. Peroxymonosulfate Activation by Photoelectroactive Nanohybrid Filter Towards Effective Micropollutant Decontamination. *Catalysts* **2022**, *12*, 416. <https://doi.org/10.3390/catal12040416>

Academic Editor: Pedro B. Tavares

Received: 15 March 2022

Accepted: 4 April 2022

Published: 7 April 2022

Publisher's Note: MDPI stays neutral with regard to jurisdictional claims in published maps and institutional affiliations.



Copyright: © 2022 by the authors. Licensee MDPI, Basel, Switzerland. This article is an open access article distributed under the terms and conditions of the Creative Commons Attribution (CC BY) license (<https://creativecommons.org/licenses/by/4.0/>).

Abstract: Herein, we report and demonstrate a photoelectrochemical filtration system that enables the effective decontamination of micropollutants from water. The key to this system was a photoelectric-active nanohybrid filter consisting of a carbon nanotube (CNT) and MIL-101(Fe). Various advanced characterization techniques were employed to obtain detailed information on the microstructure, morphology, and defect states of the nanohybrid filter. The results suggest that both radical and nonradical pathways collectively contributed to the degradation of antibiotic tetracycline, a model refractory micropollutant. The underlying working mechanism was proposed based on solid experimental evidences. This study provides new insights into the effective removal of micropollutants from water by integrating state-of-the-art advanced oxidation and microfiltration techniques.

Keywords: nanohybrid filter; photoelectrochemical filtration; carbon nanotubes; MIL-101(Fe); tetracycline

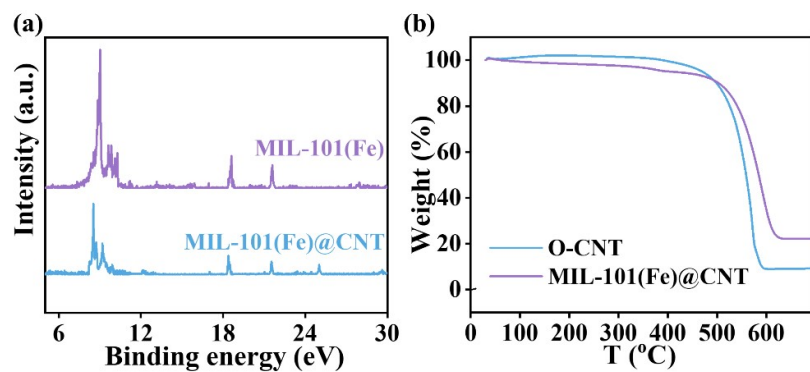


Figure S1. (a) XRD pattern and (b) TGA curves of 3 mM MIL-101(Fe)@CNT and O-CNT.

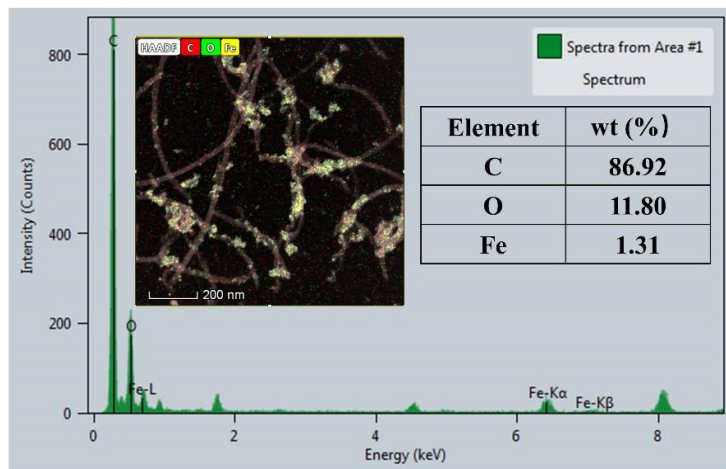


Figure S2. (a) Energy dispersive spectra of the MIL-101(Fe)@CNT filter.

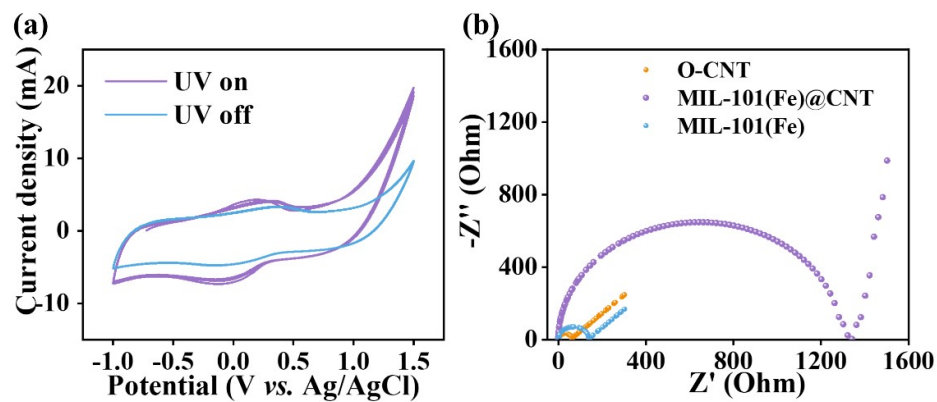


Figure S3. (a) Cyclic voltammetry curves of 3 mM MIL-101(Fe)@CNT with or without UV irradiation. (b) Nyquist diagrams of 3 mM MIL-101(Fe)@CNT and MIL-101(Fe). Environmental conditions: $[Na_2SO_4]_0 = 50$ mM.

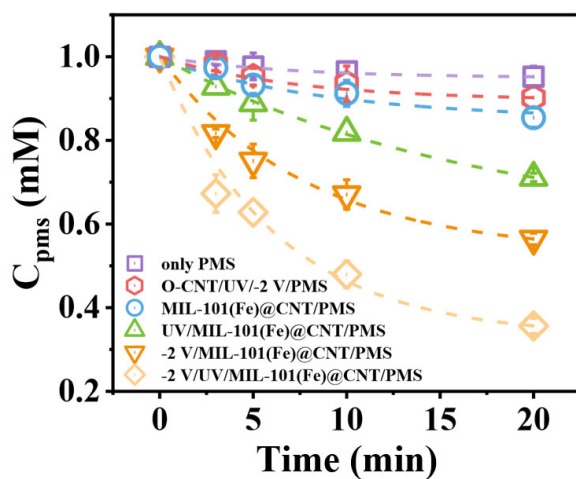


Figure S4. Residual concentration of PMS in different systems. Experimental conditions: MIL-101(Fe)@CNT = 3 mM, $[\text{TC}]_0 = 20 \text{ mg L}^{-1}$, applied voltage = -2 V, illumination voltage = 3.8 V, pH = 6.0.

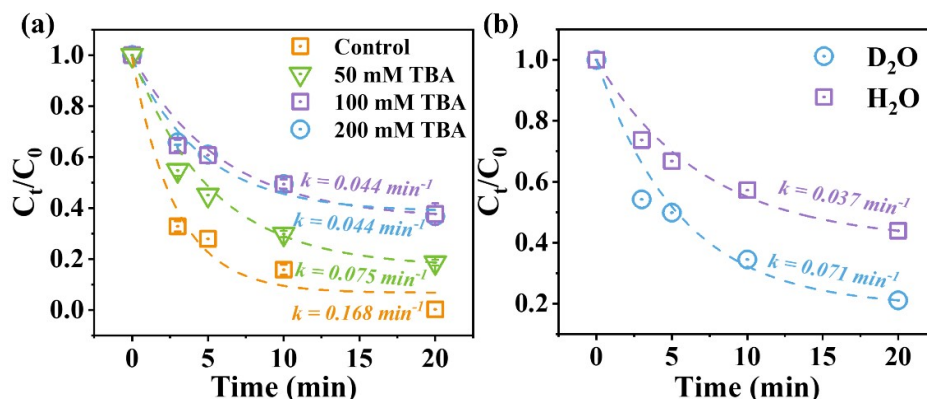


Figure S5. Effects of (a) adding TBA and (b) reaction solvent (H_2O and D_2O) on the TC degradation. Experimental conditions: MIL-101(Fe)@CNT = 3 mM, $[\text{TC}]_0 = 20 \text{ mg L}^{-1}$, applied voltage = -2 V, illumination voltage = 3.8 V, pH = 6.0.

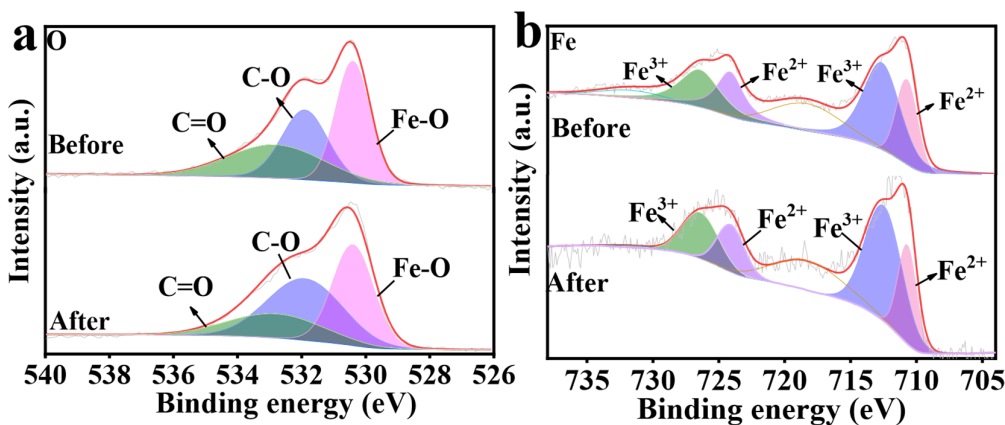


Figure S6. XPS spectra of MIL-101(Fe)@CNT: (a) O 1s and (b) Fe 2p before and after reaction.

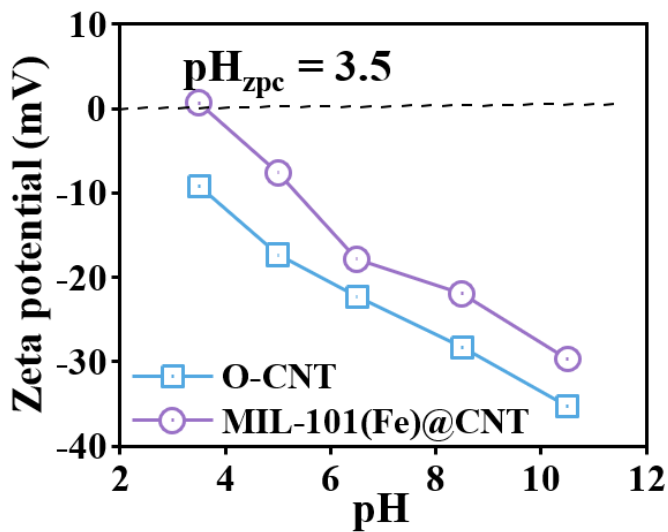


Figure S7. Zeta spectra of 3 mM MIL-101(Fe)@CNT and O-CNT.

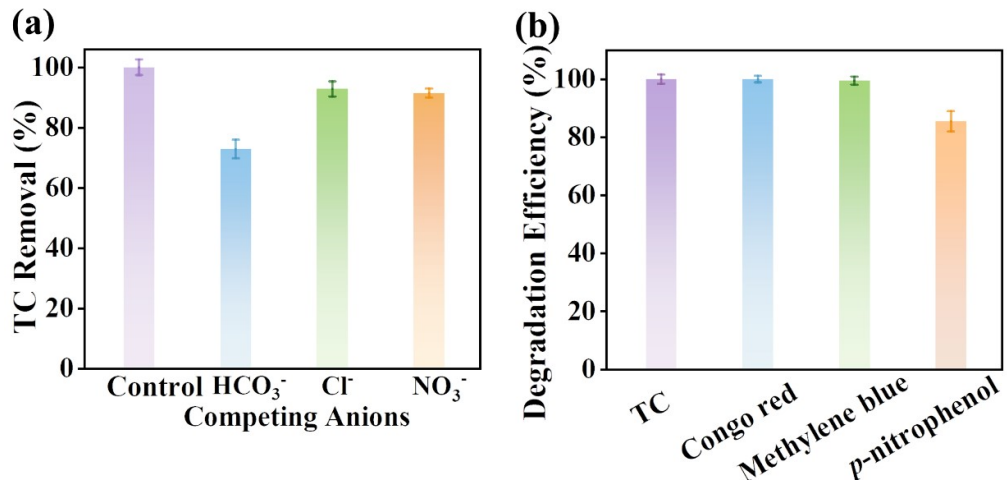


Figure S8. (a) Effect of coexisting ions on TC degradation and (b) degradation efficiency of four typical organic compounds by MIL-101(Fe)@CNT filter in circulation mode. Experimental conditions: $[\text{Congo red}]_0 = [\text{Methylene blue}]_0 = 20 \text{ mg L}^{-1}$, $[p\text{-nitrophenol}]_0 = 10 \text{ mg L}^{-1}$, MIL-101(Fe)@CNT = 3 mM, $[\text{TC}]_0 = 20 \text{ mg L}^{-1}$, applied voltage = -2 V, illumination voltage = 3.8 V, pH = 6.0.

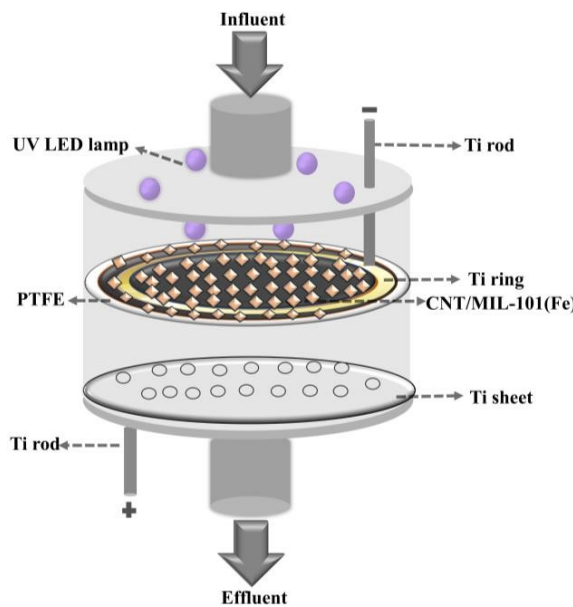


Figure S9. Schematic illustration of photoelectric reactor device.

Table S1. Corresponding k value to TC degradation in different systems according to the pseudo first order kinetic model.

Systems	C/C ₀		CPMS	
	k (min ⁻¹)	R ²	k (min ⁻¹)	R ²
PMS	0.007	0.9378	0.002	0.9143
O-CNT/-2 V/UV/PMS	0.014	0.9002	0.005	0.9330
MIL-101(Fe)@CNT/PMS	0.021	0.9046	0.008	0.9545
UV/MIL-101(Fe)@CNT/PMS	0.031	0.9203	0.017	0.9861
-2 V/MIL-101(Fe)@CNT/PMS	0.044	0.9409	0.026	0.9046
-2 V/UV/MIL-101(Fe)@CNT/PMS	0.174	0.9849	0.047	0.9080

Table S2. Corresponding k value to TC degradation in different quenchers according to the pseudo first order kinetic model.

Concentration	Methanol		TBA		L-his	
	k (min ⁻¹)	R ²	k (min ⁻¹)	R ²	k (min ⁻¹)	R ²
0 mM	0.147	0.9517	0.168	0.9696	0.178	0.9546
50 mM	0.077	0.9005	0.075	0.9076	0.056	0.9085
100 mM	0.028	0.9630	0.044	0.9034	0.036	0.9025
200 mM	0.027	0.9382	0.043	0.9152	0.034	0.9332

Table S3. XPS results of O1s.

MIL-101(Fe)@CNT	O 1s	C=O/C O/Fe O
		Relative Intensity
C=O	C-O	Fe-O
	Before	533.1 eV
	After	533.1 eV

Table S4. XPS results of Fe 2p.

	Fe 2p _{3/2}		Fe 2p _{1/2}		Fe ³⁺ /Fe ²⁺
MIL-101(Fe)@CNT					Relative Intensity
Before	712.6 eV	Fe ²⁺	726.4 eV	Fe ²⁺	0.49/0.31
After	712.5 eV	710.7 eV	726.4 eV	724.1 eV	0.59/0.21

Table S5. Corresponding *k* value to TC degradation of different operational parameters according to the pseudo first order kinetic model.

Operational parameters	Variable	<i>k</i> (min ⁻¹)	R ²
Loading	1.5 mM	0.053	0.9097
	3 mM	0.179	0.9913
	4.5 mM	0.072	0.9086
Voltage	-0.5 V	0.039	0.9021
	-1.5 V	0.066	0.9016
	-2 V	0.159	0.9563
	-2.5 V	0.082	0.9029
	3	0.085	0.9534
pH value	6	0.166	0.9544
	9	0.069	0.9683
	Batch	0.031	0.9723
Flow rate	1 mL min ⁻¹	0.057	0.9685
	2 mL min ⁻¹	0.066	0.9034
	3 mL min ⁻¹	0.158	0.9573
	4 mL min ⁻¹	0.079	0.9059
PMS concentration	0 mM	0.006	0.9763
	0.25 mM	0.028	0.9110
	0.5 mM	0.051	0.9113
	1 mM	0.181	0.9800
	1.5 mM	0.084	0.9184

Table S6. Characteristics of different water samples and corresponding *k* value to TC degradation.

Water sample	<i>k</i> (min ⁻¹)	R ²	pH	TOC (mg L ⁻¹)
DI Water	0.168	0.9878	6.5	0
Tap Water	0.137	0.9678	7.5	1.6
Lake Water	0.090	0.9448	7.7	68.3
WWTP Water	0.058	0.9113	7.1	160.1